

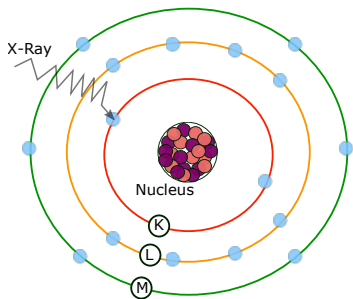
Development and Applications of Orthogonality Constrained Density Functional Theory for the Accurate Simulation X-Ray Absorption Spectroscopy

Wallace Derricotte

Dissertation Defense

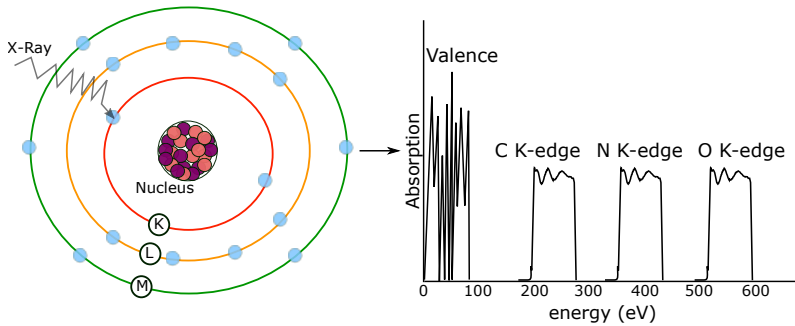
June 28th, 2017

X-ray Absorption Mechanism: Core-Excited States



- X-ray photons excite core electrons (i.e. 1s, 2s, 2p)
- Core orbitals are close to nuclei, experience strong Coulombic attraction

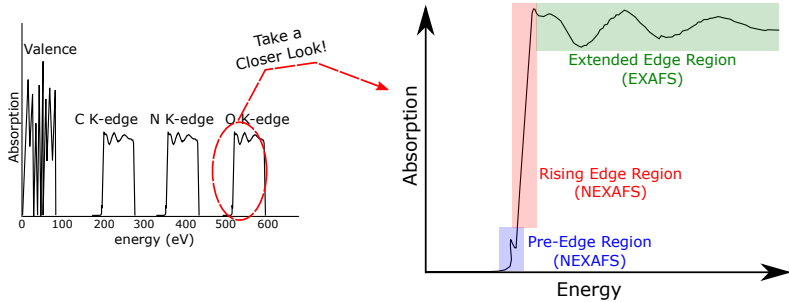
X-ray Absorption Mechanism: Core-Excited States



- X-ray photons excite core electrons (i.e. 1s, 2s, 2p)
- Core orbitals are close to nuclei, experience strong Coulombic attraction
- Produces **element specific** edge jump in absorption spectrum
 - ▶ X-ray notation based on principal quantum number¹ (K=1, L=2, M=3)

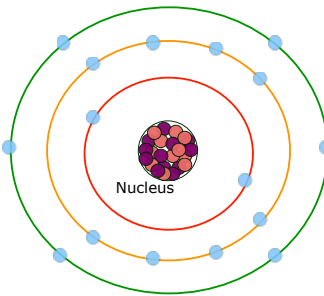
¹J. Stöhr, *NEXAFS Spectroscopy*, vol. 25. Berlin: Springer, 1992

Fine Structure of the XAS Edge



- Edge has 3 distinct regions: Pre, Rising, and Extended Edges
- Near-edge X-ray absorption fine structure (NEXAFS) spectroscopy studies the pre and rising edge regions
- Extended-edge X-ray absorption fine structure (EXAFS) spectroscopy studies the extended edge region¹

Theoretical Challenges: Orbital Relaxation

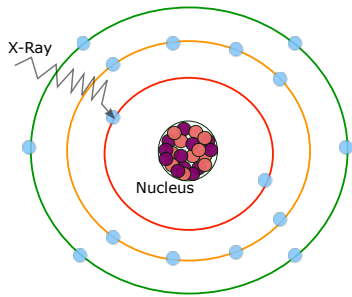


- Effective nuclear charge (Z_{eff}) on any electron can be approximated as:

$$Z_{\text{eff}} = Z - \sigma \quad (1)$$

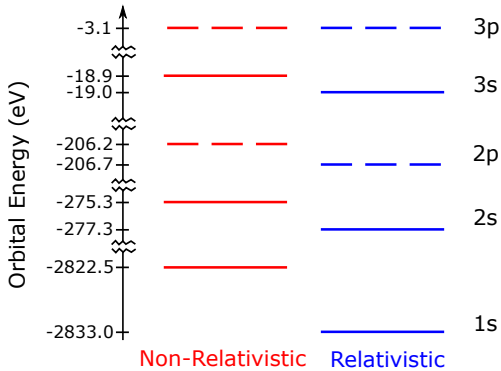
- where Z is the number of protons and σ is the average number of electrons b/w the nucleus and the electron in question

Theoretical Challenges: Orbital Relaxation



- Generation of a core-hole causes a decrease in the shielding of the nuclei
- Causes significant rearrangement in all higher lying orbitals, known as **orbital relaxation**
- It was shown that for a C atom, this effect can be on the order of 12-15 eV

Theoretical Challenges: Relativistic Effects



Orbital energies of Cl^- from non-relativistic and scalar relativistic Hartree–Fock calculations.

- Core orbitals experience large **relativistic** contraction while the valence orbitals remain relatively unaffected
- Results in increase in core-excitation energy

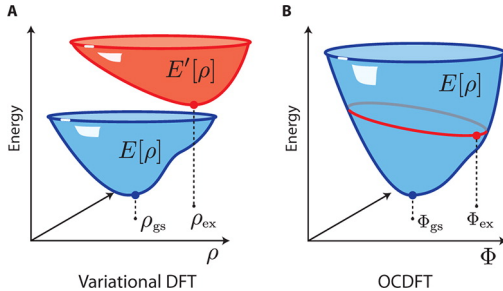
Theoretical Challenges: Relativistic Effects

Table 1: Non-relativistic (NR) and relativistic (R) energies (in eV) of the lowest lying core orbital and lowest unoccupied molecular orbital (LUMO) of water (H_2O) and silane (SiH_4) molecules calculated using spin-unrestricted Hartree–Fock (UHF) with the 3-21G basis set. Scalar relativistic effects are included by use of the 2nd order Douglas-Kroll-Hess Hamiltonian.¹ All calculations were performed using the ORCA software package.

| | H_2O | | SiH_4 | |
|--------|----------------------|------|----------------|------|
| | O 1s | LUMO | Si 1s | LUMO |
| NR-UHF | −555.88 | 7.17 | −1858.20 | 5.02 |
| R-UHF | −556.34 | 7.16 | −1863.04 | 5.03 |

- Effect is more pronounced in heavier elements
- Small but non-negligible effect on light elements

Orthogonality Constrained Density Functional Theory

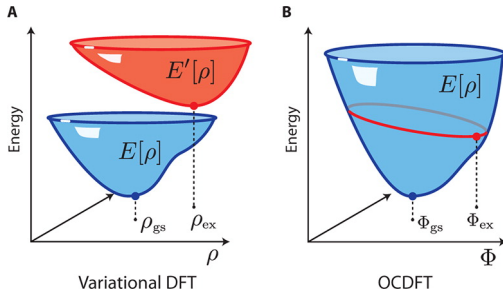


- Variational time-independent (TI) formulation of density functional theory (DFT)
- Builds upon TI-DFT methods by enforcing orthogonality between the ground and excited states

$$\langle \Phi^{(m)} | \Phi^{(n)} \rangle = \delta_{mn} \quad (2)$$

- This choice of constraint prevents **variational collapse** of the excited state SCF

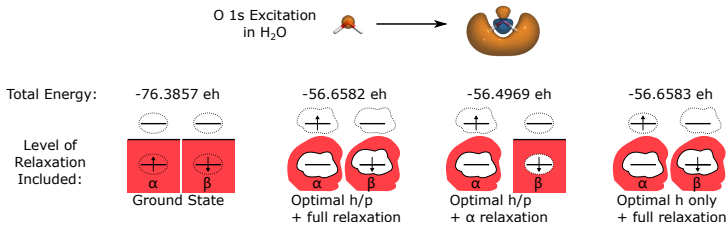
Orthogonality Constrained Density Functional Theory



- OCDFT introduces a quasi-adiabatic approximation where the excited state exchange-correlation (XC) functional is approximated as the ground state functional

$$E_{\text{OCDFT}}^{(n)}[\{\phi_i^{(n)}\}] = \sum_{\mu\nu} D_{\mu\nu}^{(n)}(T_{\mu\nu} + V_{\mu\nu}) + E_{\text{coul}}[\rho^{(n)}] + E_{\text{xc}}^{(0)}[\rho^{(n)}]. \quad (3)$$

Why OCDFT? Treatment of Orbital Relaxation



First O 1s core excitation in H₂O calculated using orthogonality constrained density functional theory at the B3LYP/3-21G level of theory. Numbers reported are the total energy of the ground state and respective core excited state calculated with varying degrees of orbital relaxation included.

- OCDFT is a Δ SCF approach and thus explicitly accounts for orbital relaxation effects
- Neglecting relaxation of β -orbitals has effect of ≈ 5 eV

Why OCDFT? Variational Stability and Computational Efficiency

Extension of OCDFT For NEXAFS Spectral Simulation

- Must introduce two new features to OCDFT to calculate NEXAFS spectra
 - ▶ Previous implementation starts from *highest lying* hole orbital (highest hole eigenvalue) however for core excitations we need to select the *lowest lying* hole orbital (lowest hole eigenvalue)
 - ▶ Algorithm must be generalized to multiple excited states

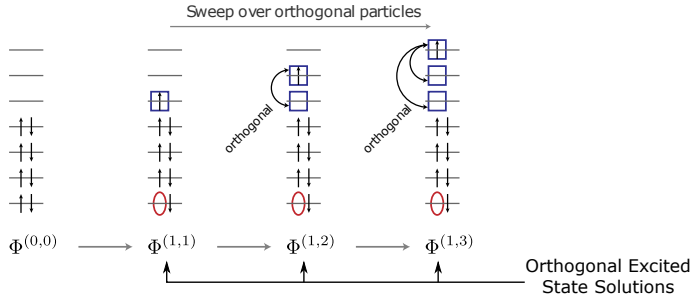
Extension of OCDFT For NEXAFS Spectral Simulation

—
—
—
↑↑
↑↑
↑↑
↑↑

$\Phi^{(0,0)}$
↑
Ground State
Determinant

- First, perform a ground state DFT calculation to obtain the ground state determinant $\Phi^{(0,0)}$
- Utilizing notation $\Phi^{(i,a)}$ where i and a are hole and particle indices respectively

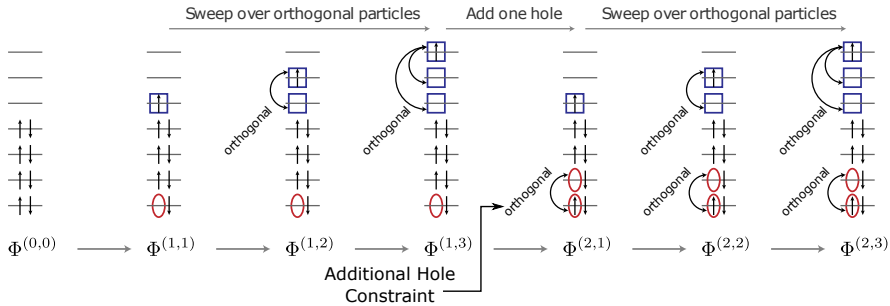
Extension of OCDFT For NEXAFS Spectral Simulation



- Perform a sweep of n_u particle orbitals to produce a series of core-excited solutions: $\Phi^{(1,1)}, \Phi^{(1,2)}, \dots, \Phi^{(1,n_u)}$.
- Characterized by particle orbitals that produce an orthogonal set:

$$\langle \phi_p^{(1,a)} | \phi_p^{(1,b)} \rangle = \delta_{ab}, \quad \forall a, b \leq n_u. \quad (4)$$

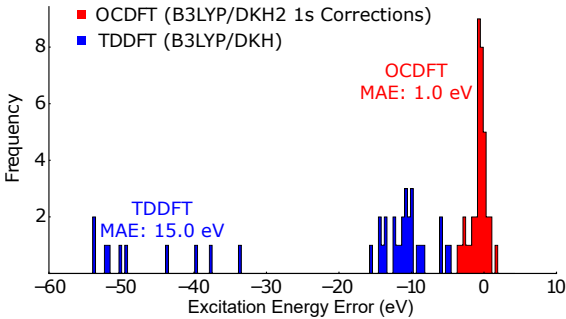
Extension of OCDFT For NEXAFS Spectral Simulation



- Increase core index by one and sweep through another series of core-excited solutions: $\Phi^{(2,1)}, \Phi^{(2,2)}, \dots, \Phi^{(2,n_u)}$.
- Where an additional constraint is added to the hole orbital to be orthogonal to the hole orbital of the first sweep:

$$\langle \phi_h^{(1,1)} | \phi_h^{(2,a)} \rangle = 0, \quad \forall a \leq n_u. \quad (5)$$

Core-Excited State Benchmark Test Set



- Max Errors:
 - ▶ OCDFT: -3.7 eV
 - ▶ TDDFT: -53.6 eV
- MAE of Other Methods:
 - ▶ EOM-CCSD: 0.9 eV
 - ▶ SOS-CIS(D): 1.2 eV

Full NEXAFS Spectral Simulation: Thymine

- Transition dipole moments (TDMs) are approximated using the Kohn–Sham determinants as:

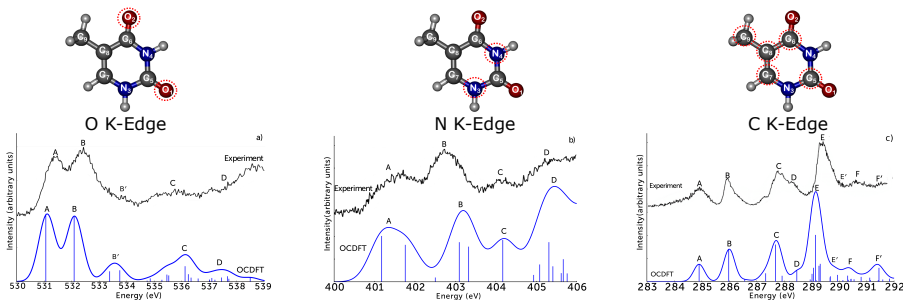
$$\mu_{n0} = \langle \Phi^{(n)} | \hat{\mathbf{r}} | \Phi^{(0)} \rangle \quad (6)$$

- Using the approximate TDMs we can compute an oscillator strength for each transition

$$f_{\text{osc}} = \frac{2}{3} |\mu_{n0}|^2 \omega_n \quad (7)$$

- Compute 10 excitations per hole for each C, N, O 1s orbital in thymine
- Spectra plotted using Gaussians with FWHM of 0.1 eV - 0.4 eV in order to simulate natural spectroscopic broadening effects.

Full NEXAFS Spectral Simulation: Thymine



- *Unshifted* OCDFT excitation energies provide excellent comparison to experiment
- Average error of 0.3 eV overall compared to experimental peak maxima

Goal of Two-Component Hamiltonians

- Full Dirac Relativistic equation involves a 4 component Hamiltonian (h^D), 2 *large* components (L), 2 *small* components (S)

$$h^D = \begin{pmatrix} h_{LL} & h_{LS} \\ h_{SL} & h_{SS} \end{pmatrix} \quad (8)$$

- Idea is to decouple large and small components of Dirac Hamiltonian through a Foldy-Wouthuysen (FW) unitary transformation to block diagonalize h^D

$$U^\dagger h^D U = U^\dagger \begin{pmatrix} h_{LL} & h_{LS} \\ h_{SL} & h_{SS} \end{pmatrix} U = \begin{pmatrix} h_{++}^{\text{FW}} & 0 \\ 0 & h_{--}^{\text{FW}} \end{pmatrix} \quad (9)$$

- The positive energy contribution is then isolated, which is a sum of relativistic kinetic (T^{rel}) and potential (V^{rel})

$$h_{++}^{\text{FW}} = T^{\text{rel}} + V^{\text{rel}} \quad (10)$$

Spin-Free Modified Dirac Equation

- Following FW Unitary transformation, the one-electron Dirac equation can be written as:

$$\begin{pmatrix} V & T \\ T & \frac{W}{4c^2} - T \end{pmatrix} \begin{pmatrix} C^L \\ C^S \end{pmatrix} = \begin{pmatrix} S & 0 \\ 0 & \frac{T}{2c^2} \end{pmatrix} \begin{pmatrix} C^L \\ C^S \end{pmatrix} E \quad (11)$$

- Where W is the relativistic potential which is the sum of spin-free (SF) and spin-orbit (SO) contributions:

$$W = W^{\text{SF}} + W^{\text{SO}} \quad (12)$$

- Neglecting the SO term yields the **spin-free** version of the modified Dirac equation, in AO basis (χ_μ) W^{SF} is

$$W_{\mu\nu}^{\text{SF}} = \langle \chi_\mu | \hat{p} \cdot (\hat{V} \hat{p}) | \chi_\nu \rangle \quad (13)$$

eXact-Two-Component Hamiltonian (X2C)

- Given the form of the unitary transformation of the Dirac Hamiltonian

$$U^\dagger h^D U = \begin{pmatrix} h_{++}^{\text{FW}} & 0 \\ 0 & h_{--}^{\text{FW}} \end{pmatrix}, U = \begin{pmatrix} 1 & -X^\dagger \\ X & 1 \end{pmatrix} \begin{pmatrix} R & 0 \\ 0 & R \end{pmatrix} \quad (14)$$

- X and R are the *coupling* and *renormalization* matrices respectively and relate the MO coefficients of the 2c wavefunction

$$C^S = XC^L \quad C^L = RC^{2c} \quad (15)$$

- In X2C, these relations are used to build the relativistic kinetic and potential energy operators

$$T^{X2C} = R^\dagger(TX + X^\dagger T - X^\dagger TX)R \quad (16)$$

$$V^{X2C} = R^\dagger(V + \frac{1}{4c^2}X^\dagger W^{\text{SF}} X)R \quad (17)$$

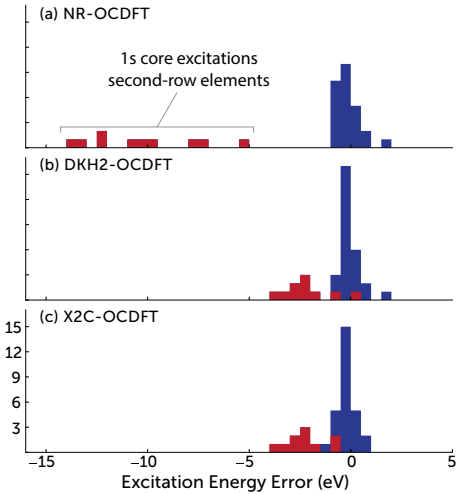
X2C-OCDFT

- The *relativistic* X2C kinetic and potential terms are now included in the OCDFT energy functional

$$E_{\text{OCDFT}}^{(n)}[\{\phi_i^{(n)}\}] = \sum_{\mu\nu} D_{\mu\nu}^{(n)}(T_{\mu\nu}^{\text{X2C}} + V_{\mu\nu}^{\text{X2C}}) + E_{\text{coul}}[\rho^{(n)}] + E_{\text{xc}}^{(0)}[\rho^{(n)}]. \quad (18)$$

- X2C one-electron operator is formed before the SCF cycle and added to the *nonrelativistic* two-electron operators

X2C-OCDFT Benchmark



- Benchmarked using 37 core-excitations from 13 different molecules
- Calculations done using B3LYP functional and fully uncontracted aug-cc-pVDZ basis set
- MAE for X2C-OCDFT:
 - ▶ 1st row: 0.3 eV
 - ▶ 2nd row: 0.7 eV

Relativistic Effects vs. Correlation Effects

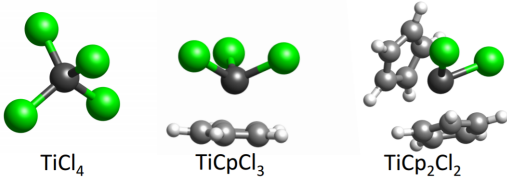
| Transitions | Relativistic (eV) | Correlation (eV) |
|---------------|-------------------|------------------|
| First row 1s | 0.2 | 0.6 |
| Second row 1s | 8.0 | 3.4 |
| Second row 2p | 0.5 | 1.1 |
| All | 2.2 | 1.3 |

$$\text{Rel} = \text{OCDFT}^{\text{NR}}(E_{\text{xc}}^{\text{B3LYP}}) - \text{OCDFT}^{\text{X2C}}(E_{\text{xc}}^{\text{B3LYP}}) \quad (19)$$

$$\text{Corr} = \text{OCDFT}^{\text{X2C}}(E_{\text{xc}}^{\text{B3LYP}}) - \text{OCDFT}^{\text{X2C}}(E_{\text{x}}^{\text{HF}}) \quad (20)$$

- Proper treatment of electron correlation is more important for 1st row elements
- Quickly outpaced by relativistic effects for 2nd row
- Proper treatment of relativistic effects will be extremely important for transition metals

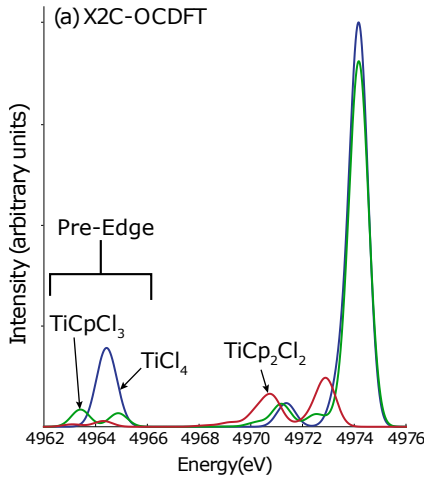
K-Edge of Tetracoordinated Ti Complexes



| State | TDDFT | | OCDFT | | Exp. |
|-------|--------|-------|-------|------|------|
| | NR | DKH2 | NR | X2C | |
| 1 | -107.9 | -78.6 | -35.6 | -5.0 | |
| 2 | -107.9 | -78.6 | -35.5 | -4.5 | |
| 3 | -107.0 | -77.6 | -36.4 | -5.7 | |
| 4 | -106.9 | -77.6 | -35.3 | -4.8 | |
| 5 | -107.0 | -77.7 | -36.3 | -5.7 | |

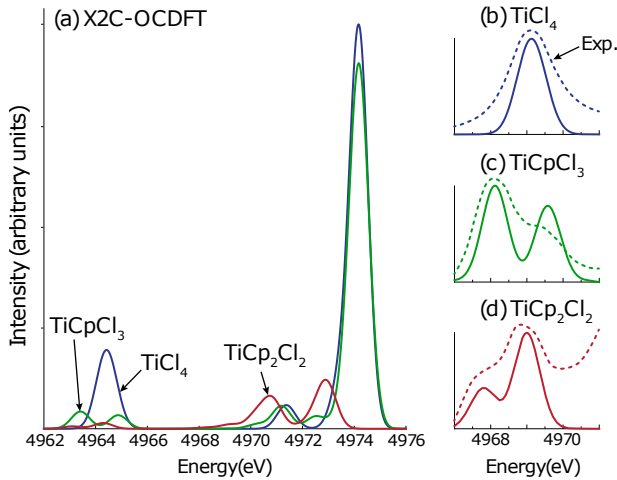
- Pre-edge feature is calculated within ≈ 5.0 eV of experiment

Pre-edge Features of Tetracoordinated Ti Complexes



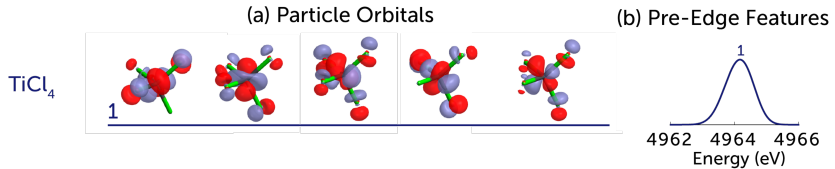
- Pre-edge intensity drop after adding Cp rings to coordination

Pre-edge Features of Tetracoordinated Ti Complexes



- Peak splitting of pre-edge after adding Cp rings to coordination

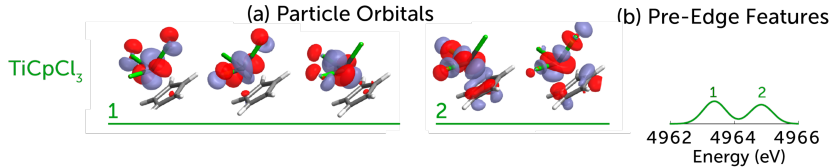
Particle Orbital Analysis of Pre-Edge TiCl_4



| State | TiCl_4 | f |
|-------|-----------------|--------|
| | Energy | |
| 1 | 4964.2 | 0.0945 |
| 2 | 4964.7 | 0.0940 |
| 3 | 4963.5 | 0.0002 |
| 4 | 4964.4 | 0.0947 |
| 5 | 4963.5 | 0.0000 |

- All particle orbitals have similar character (i.e. Ti d and Cl p)

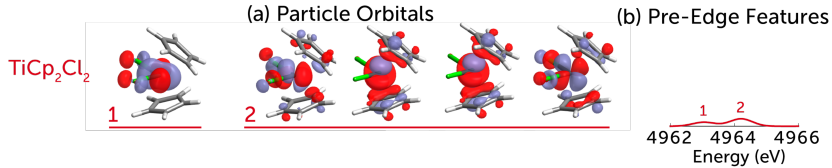
Particle Orbital Analysis of Pre-Edge TiCpCl_3



| State | TiCpCl_3 | |
|-------|-------------------|----------|
| | Energy | <i>f</i> |
| 1 | 4963.4 | 0.0202 |
| 2 | 4963.4 | 0.0191 |
| 3 | 4963.5 | 0.0164 |
| 4 | 4964.9 | 0.0220 |
| 5 | 4963.9 | 0.0217 |

- States with significant Cp ring contributions are pushed to higher energy

Particle Orbital Analysis of Pre-Edge TiCp_2Cl_2



| State | TiCp_2Cl_2 | |
|-------|----------------------------|----------|
| | Energy | <i>f</i> |
| 1 | 4963.1 | 0.0078 |
| 2 | 4964.3 | 0.0121 |
| 3 | 4964.4 | 0.0009 |
| 4 | 4964.4 | 0.0000 |
| 5 | 4964.3 | 0.0055 |

- States with significant Cp ring contributions are pushed to higher energy

Further Investigation of Pre-Edge Intensity

- Pre-edge intensity will be evaluated using the following methods:
 - ▶ Natural population analysis using JANPA software
 - ▶ Atomic decomposition of the total dipole moment
- We can decompose the total dipole moment in the following fashion

$$\mu_{0n} = \langle \Phi^{(n)} | \hat{\mathbf{r}} | \Phi^{(0)} \rangle = \sum_{\mu\nu} D_{\mu\nu}^{0n} \langle \chi_\mu | \hat{\mathbf{r}} | \chi_\nu \rangle \quad (21)$$

- From here we can do a restricted sum over donor/acceptor atom and angular momentum shell

$$\mu_{0n}(A_{l_A} \rightarrow B_{l_B}) = \sum_{\mu \in A_{l_A}} \sum_{\nu \in B_{l_B}} D_{\mu\nu}^{0n} \langle \chi_\mu | \mathbf{r} | \chi_\nu \rangle \quad (22)$$

Further Investigation of Pre-Edge Intensity

Natural Population Analysis

| State | ΔT_{Ip} | | | $\Delta \text{Cl}_{\text{p}}$ | | | ΔT_{d} | | |
|-------|------------------------|-------------------|----------------------------|-------------------------------|-------------------|----------------------------|-----------------------|-------------------|----------------------------|
| | TiCl_4 | TiCpCl_3 | TiCp_2Cl_2 | TiCl_4 | TiCpCl_3 | TiCp_2Cl_2 | TiCl_4 | TiCpCl_3 | TiCp_2Cl_2 |
| 1 | 0.0107 | 0.0066 | 0.0097 | -0.2184 | -0.0597 | 0.0051 | 1.1348 | 1.1614 | 1.2586 |

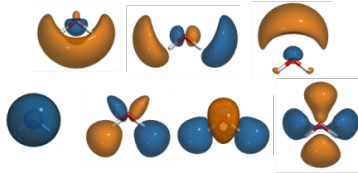
Atomic Decomposition of Dipole Moments

| Contribution | μ_x | μ_y | μ_z | $ \mu $ |
|---------------------------------------|-----------|-----------|-----------|----------|
| State 1 | | | | |
| $\text{Ti}_s \rightarrow \text{Ti}_p$ | -0.000395 | -0.000079 | -0.000113 | 0.000418 |
| $\text{Cl}_p \rightarrow \text{Cl}_p$ | +0.000062 | +0.000012 | +0.000018 | 0.000066 |
| $\text{Ti}_s \rightarrow \text{Cl}_p$ | -0.000006 | +0.000003 | -0.000064 | 0.000064 |
| Other | -0.000007 | +0.000002 | +0.000073 | 0.000073 |

- Population analysis shows that the transitions are $1s \rightarrow 3d$
- Largest dipole contribution is $\text{Ti}_s \rightarrow \text{Ti}_d$

Localized Intrinsic Valence Virtual Orbitals

(A) Canonical molecular orbitals (CMOs)

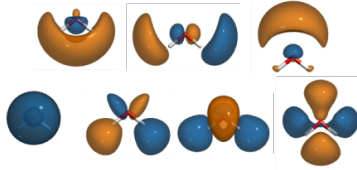


- Start with a set of virtual canonical molecular orbitals (CMOs) expanded in an atom-centered basis $\{\chi_\mu\}$

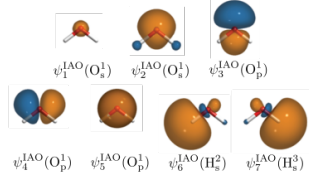
$$|\phi_a\rangle = \sum_{\mu}^{N_{AO}} |\chi_{\mu}\rangle C_{\mu a}, \quad a = 1, \dots, N_{vir} \quad (23)$$

Localized Intrinsic Valence Virtual Orbitals

(A) Canonical molecular orbitals (CMOs)



(B) Intrinsic atomic orbitals (IAOs)

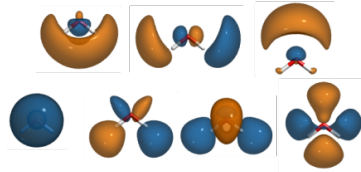


- Evaluate overlap (S) with set of Intrinsic Atomic Orbitals (IAOs)

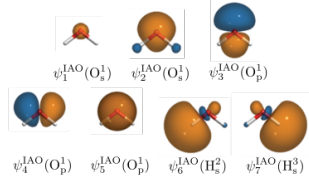
$$(S)_{a\rho} = \langle \phi_a | \psi_\rho^{\text{IAO}} \rangle \quad (24)$$

Localized Intrinsic Valence Virtual Orbitals

(A) Canonical molecular orbitals (CMOs)



(B) Intrinsic atomic orbitals (IAOs)

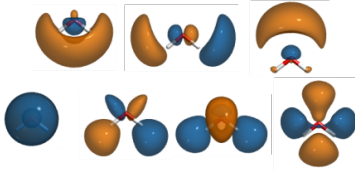


- Perform SVD of overlap matrix to get orthogonal transformation matrices \mathbf{U} and \mathbf{V}

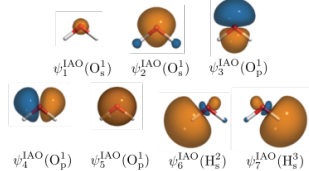
$$\mathbf{S} = \mathbf{U}\sigma\mathbf{V}^\dagger \quad (25)$$

Localized Intrinsic Valence Virtual Orbitals

(A) Canonical molecular orbitals (CMOs)



(B) Intrinsic atomic orbitals (IAOs)



LIMO Procedure

A) and (B)

SVD of overlap matrix

(C) Valence virtual orbitals (VVOs)

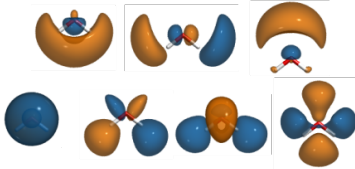


- Use U to transform canonical virtuals into valence viratual orbitals (VVOs):

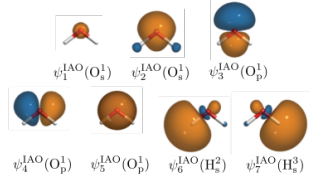
$$|\psi_v^{\text{VVO}}\rangle = \sum_a^{N_{\text{vir}}} |\phi_a\rangle U_{av}, \quad v = 1, \dots, N_{\text{VVO}}. \quad (26)$$

Localized Intrinsic Valence Virtual Orbitals

(A) Canonical molecular orbitals (CMOs)



(B) Intrinsic atomic orbitals (IAOs)



LIVO Procedure

(A) and (B)

SVD of overlap matrix

(C) Valence virtual orbitals (VVOs)



Pipek-Mezey Localization

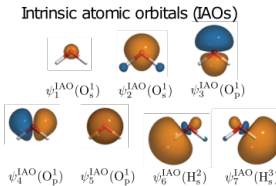
(D) Localized intrinsic VVOs (LIVVOs)



- Pipek-Mezey localization can be employed in order to yield an orbital set that represents each valence antibonding interaction in the molecular environment

Determining Atomic Character of IAOs

- Atomic character is assigned using a Mulliken Population Analysis



Gross Populations

| A_l | ψ_1^{IAO} | ψ_2^{IAO} | ψ_3^{IAO} | ψ_4^{IAO} | ψ_5^{IAO} | ψ_6^{IAO} | ψ_7^{IAO} |
|----------------|-----------------------|-----------------------|-----------------------|-----------------------|-----------------------|-----------------------|-----------------------|
| O_s^1 | 1.00 | 1.16 | 0.00 | 0.00 | 0.00 | -0.08 | -0.08 |
| O_p^1 | 0.00 | 0.00 | 1.04 | 1.11 | 1.00 | -0.07 | -0.07 |
| H_s^2 | 0.00 | -0.08 | -0.02 | -0.05 | 0.00 | 1.18 | -0.03 |
| H_s^3 | 0.00 | -0.08 | -0.02 | -0.05 | 0.00 | -0.03 | 1.18 |

- We compute the population matrix ($P_{\mu\nu}$) as:

$$P_{\mu\nu}(\rho) = \tilde{C}_{\mu\rho} S_{\mu\nu} \tilde{C}_{\nu\rho}, \quad \rho = 1, \dots, N_{\text{IAO}} \quad (27)$$

- Gross populations on each atom A and angular momentum shell l are obtained via partial sums of $P_{\mu\nu}$

$$\text{GP}_{A_l}(\rho) = \sum_{\mu \in A_l} \sum_{\nu}^{N_{\text{AO}}} P_{\mu\nu}(\rho) \quad (28)$$

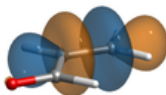
- character of each IAO chosen as maximum $\text{GP}_{A_l}(\rho)$ contribution

Using IAOs to Classify LIVVOs

- Overlap of each LIVVO (ψ_l^{LIVVO}) with the IAOs (ψ_ρ^{IAO}) is evaluated:

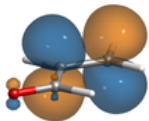
$$S'_{l\rho} = |\langle \psi_l^{\text{LIVVO}} | \psi_\rho^{\text{IAO}} \rangle|^2 \quad (29)$$

- Assign orbital character (σ, π, \dots) of LIVVOs based on atomic character (s,p, \dots) of IAOs



$$= 0.20 \psi^{\text{IAO}}(\text{C}_s^2) + 0.24 \psi^{\text{IAO}}(\text{C}_p^2)$$

$$+ 0.20 \psi^{\text{IAO}}(\text{C}_s^3) + 0.25 \psi^{\text{IAO}}(\text{C}_p^3) = \sigma_{\text{C}^2-\text{C}^3}^*$$

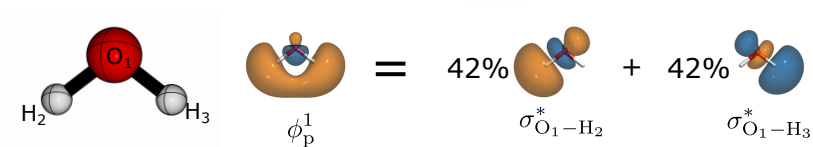


$$= 0.47 \psi^{\text{IAO}}(\text{C}_p^2) + 0.51 \psi^{\text{IAO}}(\text{C}_p^3) = \pi_{\text{C}^2-\text{C}^3}^*$$

Assigning Orbital Character of OCDFT Particle Orbitals

- Character of the particle orbital $\phi_p^{(n)}$ by evaluating its overlap with each LIVVO (ψ_l^{LIVVO})

$$\Omega_{pl}^{(n)} = |\langle \phi_p^{(n)} | \psi_l^{\text{LIVVO}} \rangle|^2. \quad (30)$$

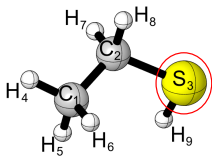


- Total valence character can be quantified by summing all LIVVO contributions. (84% for above H_2O example)

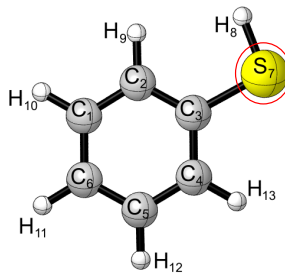
$$t_{\text{p}}^{\text{val},(n)} = \sum_l^{N_{\text{LIVVO}}} \Omega_{pl}^{(n)}. \quad (31)$$

Assigning Transitions in S K-edge of Ethanethiol and Benzenethiol

- Spectra are calculated with OCDFT at the B3LYP/jun-cc-pVTZ level of theory

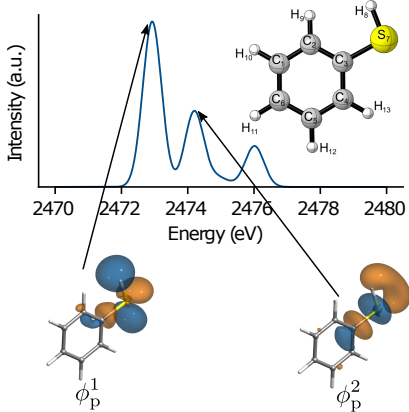
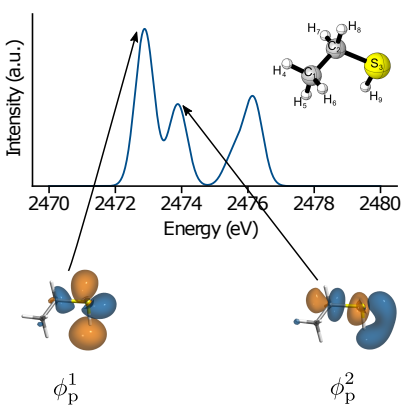


Ethanethiol



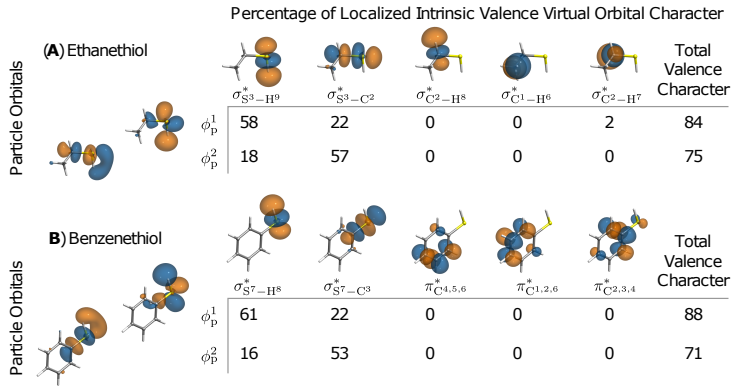
Benzenethiol

What are the local contributions to ϕ_p^1 and ϕ_p^2 ?



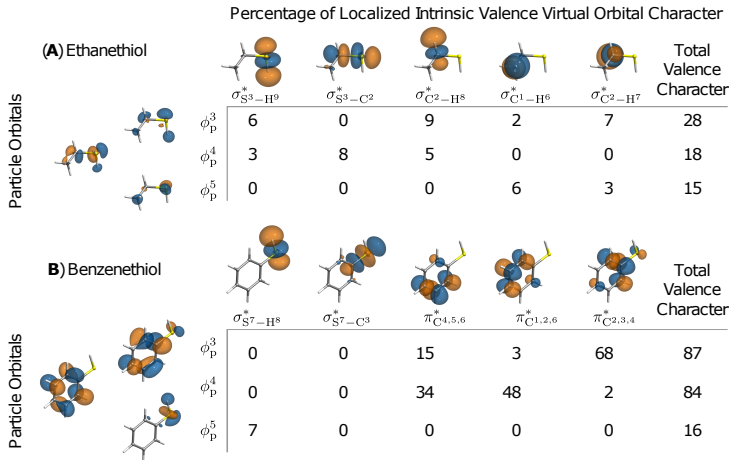
- Particle orbitals contain orbital character along S – C and S – H
- What is the contribution of the thiol bond to each excited state?

What are the local contributions to ϕ_p^1 and ϕ_p^2 ?



- LIVVO analysis yields *unambiguous* assignment for each particle orbital
- Thiol bond is large contributor to first peak, weak contributor to second peak

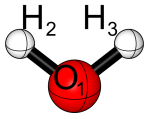
Other Contributions to the S K-Edge



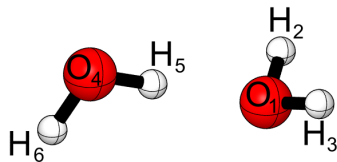
- ϕ_p^3 and ϕ_p^4 localized away from S atom in benzenethiol, results in lower intensity

Effect of Hydrogen Bonding on O K-Edge of Water

- Spectra are calculated with OCDFT at the B3LYP/jun-cc-pVTZ level of theory

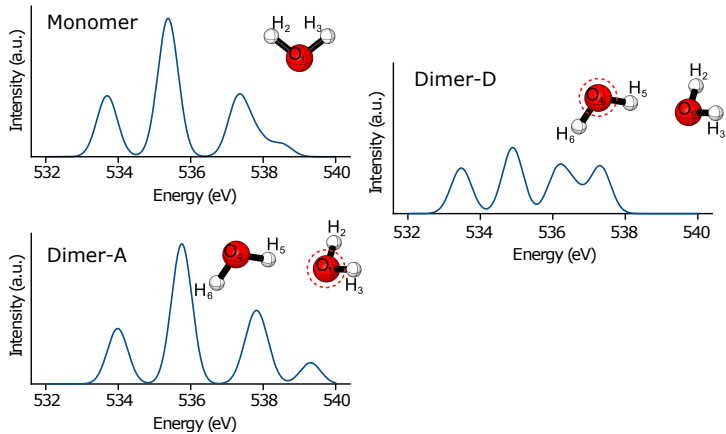


Monomer



Dimer

Effect of Hydrogen Bonding on O K-Edge of Water



- Accepting H-bond (Dimer-A) has small effect on spectral features, donating H-bond (Dimer-D) has significant effect

Effect of Hydrogen Bonding on O K-Edge of Water

Percentage of Localized Intrinsic Valence Virtual Orbital Character

(A) Water monomer

| | | | Total Valence Character |
|------------|----------------------|----------------------|-------------------------|
| | $\sigma_{O_1-H_2}^*$ | $\sigma_{O_1-H_3}^*$ | |
| ϕ_p^1 | 42 | 42 | 85 |
| ϕ_p^2 | 38 | 38 | 75 |

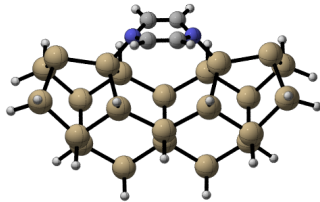
(B) Water dimer-A

| Particle Orbitals | | | | | Total Valence Character |
|-------------------|----------------------|----------------------|----------------------|----------------------|-------------------------|
| | $\sigma_{O_1-H_2}^*$ | $\sigma_{O_1-H_3}^*$ | $\sigma_{O_4-H_6}^*$ | $\sigma_{O_4-H_5}^*$ | |
| ϕ_p^1 | 41 | 41 | 0 | 0 | 84 |
| ϕ_p^2 | 39 | 39 | 0 | 0 | 77 |

(C) Water dimer-D

| | | | | | Total Valence Character |
|------------|----------------------|----------------------|----------------------|----------------------|-------------------------|
| | $\sigma_{O_1-H_2}^*$ | $\sigma_{O_1-H_3}^*$ | $\sigma_{O_4-H_6}^*$ | $\sigma_{O_4-H_5}^*$ | |
| ϕ_p^1 | 5 | 5 | 52 | 16 | 79 |
| ϕ_p^2 | 18 | 18 | 24 | 10 | 69 |

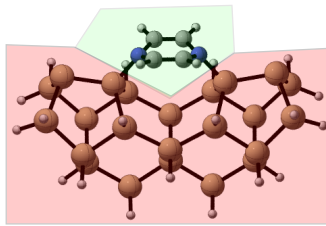
Organic Core-Excitations in Chemisorbed Molecules



Pyrazine ($C_4H_4N_2$) on Si(100)

- Appropriate surface cluster models contain at least 10 or more surface atoms

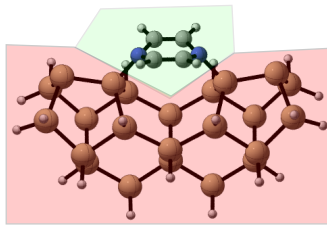
Organic Core-Excitations in Chemisorbed Molecules



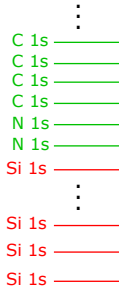
Pyrazine ($C_4H_4N_2$) on Si(100)

- Appropriate surface cluster models contain at least 10 or more surface atoms
- Model complexes contain the organic **adsorbate** attached to a **surface cluster**

Organic Core-Excitations in Chemisorbed Molecules



Pyrazine ($C_4H_4N_2$) on Si(100)



- Lowest energy core orbitals are associated with the **surface cluster**
- Presents an algorithmic challenge for original OCDFT algorithm
- Need a method to specifically target core orbitals of the **organic adsorbate**

Maximum Subspace Occupation Approach

- Consider a set of atomic orbital basis functions (φ_s) ordered by atom center, principal quantum number, and angular momentum
- We can build an operator that projects onto the AO subset

$$\hat{\Gamma}_s = \sum_s |\varphi_s\rangle\langle\varphi_s| \quad (32)$$

- Evaluate an atomic orbital occupation number (Ω_i) for each occupied molecular orbital (ϕ_i) within the desired subspace

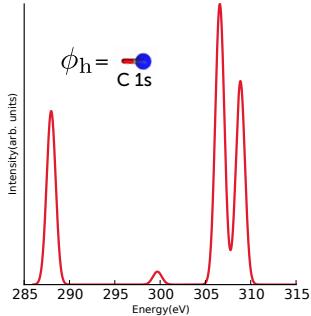
$$\Omega_i = \langle \phi_i | \hat{\Gamma}_s | \phi_i \rangle = \sum_s \langle \phi_i | \varphi_s \rangle \langle \varphi_s | \phi_i \rangle. \quad (33)$$

- Hole orbital (ϕ_h) is now chosen from a subset of the occupied orbitals where Ω_i is greater than a user-defined occupation threshold parameter

Maximum Subspace Occupation Approach: CO Example

| | ϕ_i | Ω_i |
|-----------------|----------|------------|
| 5A ₁ | | 0.008 |
| 1B ₂ | | 0.000 |
| 1B ₁ | | 0.000 |
| 4A ₁ | | 0.008 |
| 3A ₁ | | 0.007 |
| 2A ₁ | | 0.976 |
| 1A ₁ | | 0.000 |

a) Evaluate Subspace occupation of each occupied orbital for C 1s subspace



b) Hole orbital is chosen as the C 1s orbital. C K-Edge is calculated directly.

- C 1s orbital is targeted based on its occupation in the C 1s atomic orbital subset
- Note: Due to locality of core orbitals, threshold can be set fairly high